

THE EVOLUTION OF VERY LOW MASS STARS¹

L. A. NELSON, S. A. RAPPAPORT, AND P. C. JOSS

Center for Theoretical Physics, Center for Space Research, and Department of Physics,
Massachusetts Institute of Technology

Received 1986 February 18; accepted 1986 May 8

ABSTRACT

We present the results of numerical evolutionary calculations for stars with masses in the range of 0.01–0.10 M_{\odot} . We have followed the evolution of these stars from the early stages of contraction, through deuterium burning, to the very late stages of degenerate cooling at ages comparable to that of the Galaxy. By varying the assumed surface boundary conditions, we systematically explored the sensitivity of our evolutionary sequences to the major uncertainties in the input physics. We find that, at a given age, the effective temperatures and bolometric luminosities of stars with masses $\lesssim 0.06 M_{\odot}$ are quite well determined despite these uncertainties. However, the minimum mass ($\sim 0.08 M_{\odot}$) for which thermal equilibrium can be established via hydrogen burning is moderately sensitive to the assumed input physics. Our calculations are particularly appropriate to the interpretation of the observations of substellar objects such as Van Biesbroeck 8B. Specifically, we find that if VB 8B has an age in excess of $\sim 10^9$ yr, then it has a mass in the range of 0.04–0.08 M_{\odot} . We estimate the central density and temperature of VB 8B to be in the ranges of ~ 300 – 1300 g cm^{-3} and ~ 1.0 – 2.0×10^6 K, respectively. We also utilize our cooling curves to generate theoretical luminosity functions for very low mass stars.

Subject headings: stars: evolution — stars: interiors — stars: late-type

I. INTRODUCTION

There has recently been considerable renewed interest in the subject of brown dwarfs because of (i) the possibility that these objects comprise a significant fraction of the local missing mass in the Galactic disk (see, e.g., Bahcall 1984), and (ii) the recent discovery of the first bona fide brown dwarf, Van Biesbroeck 8B (VB 8B), which has an effective temperature of only ~ 1360 K (McCarthy, Probst, and Low 1985). We take, as a working definition of a brown dwarf, a star that has insufficient mass to achieve thermal equilibrium via hydrogen burning (i.e., insufficient mass to achieve main-sequence status). The actual minimum main-sequence mass depends on several factors, including the chemical composition of the star (Rappaport and Joss 1984), but it is generally agreed that for cosmic abundances, this minimum mass is $\sim 0.08 M_{\odot}$ (see, e.g., Kumar 1963a; Hoxie 1970; Grossman, Hays, and Graboske 1974, hereafter GHG; D'Antona and Mazzitelli 1985, hereafter DM). The lower mass limit for brown dwarfs is not precisely defined, but we consider here only stars with masses sufficiently high that no more than a small fraction of the stellar matter is in atomic or molecular form (i.e., masses $M \gtrsim 0.01 M_{\odot}$). We also note that $0.01 M_{\odot}$ is nearly equal to the minimum mass for which a substellar object can attain a temporary state of thermal equilibrium through the burning of a small amount of primordial deuterium (see Grossman and Graboske 1973; GHG).

In addition to VB 8B, several other stars have been suggested to have masses near or below the minimum mass for main-sequence hydrogen burning or to have effective temperatures near or below that expected for the lowest mass

main-sequence star. Examples which fall into the first category include Luyten 726–8A and B and Ross 614B (see, e.g., van de Kamp 1969; GHG; Probst 1977; Popper 1980; and references cited in these works), while the latter class of stars includes LP 271–25 = LHS 2924 and Van Biesbroeck 8A itself (see Probst and Liebert 1983). In addition, several very low mass ($\lesssim 0.01 M_{\odot}$) unseen companions to nearby stars have also been suggested on the basis of astrometric observations (van de Kamp 1975; Lippincott 1978). The reliability of these astrometric detections remains uncertain (Gatewood 1976), but several other astrometric candidates for brown dwarfs in binary systems are currently under investigation (Harrington 1986).

In addition, the presence of low-mass ($\lesssim 0.1 M_{\odot}$) stars has been inferred in several interacting binary systems, including two binary X-ray sources and several cataclysmic variables with orbital periods near the minimum in their orbital period distribution (see, e.g., Patterson 1984). In all cases, however, these binary systems are studied in X-radiation or visible light, or both, produced by the accretion of matter from the hypothesized low-mass secondary to a collapsed star (degenerate dwarf or neutron star). Furthermore, the secondary stars are thought to have attained their present low-mass state by transferring a large amount of their original mass to the collapsed star (or by loss of mass from the binary altogether). Thus, most or all of these low-mass interacting stars are probably not primordial (i.e., they have evolved from more massive objects). Theoretical studies of this type of system (see Paczyński and Sienkiewicz 1981; Rappaport, Joss, and Webbink 1982, hereafter RJW) have provided (i) an apparently successful explanation for the existence of the 80 minute minimum in the orbital period distribution of cataclysmic variables and (ii) a description of the evolution of brown dwarfs that are undergoing mass loss.

The evolutionary history of brown dwarfs can generally be divided into three phases: (i) an initial contraction stage (for ages $t \lesssim 10^6$ yr), (ii) a deuterium-burning phase (with a duration of $\lesssim 10^7$ yr), and (iii) a degenerate cooling stage. The study

¹ This work was supported in part by the National Aeronautics and Space Administration under contracts NAS5-24441 and NGL-22-009-638 and grant NSG 7643, and by the National Science Foundation under grant AST 84-19834.

of the initial contraction of brown dwarfs was pioneered by Hayashi and Nakano (1963) and Kumar (1963*b*) (see also Hoxie 1970). A more sophisticated numerical treatment of the problem, which also included the deuterium-burning phase, was carried out by Grossman and Graboske (1973) and GHG. The cooling was followed until the effective temperatures dropped to ~ 2000 K. Such effective temperatures correspond to ages of $\lesssim 3 \times 10^8$ yr (for $M \lesssim 0.05 M_\odot$), which are young compared to the age of the Galaxy. However, theoretical cooling curves extending to ages up to $\sim 10^{10}$ yr are important to the interpretation of observed brown dwarfs and can provide useful guidance in the planning of searches for such objects.

The first estimates of the properties of brown dwarfs during the late stages of degenerate cooling were made by Tarter (1975). Her estimates were based on model calculations (GHG and references therein) that she then extrapolated to lower effective temperatures ($T_e < 1200$ K) and later ages than were covered by the models. Stevenson (1978) carried out the first semi-analytical calculations of the cooling of brown dwarfs to very low temperatures and old ages, but subject to the constraint of an exactly constant stellar radius (in the limit of high degeneracy). More recently, Nelson, Rappaport, and Joss (1985; hereafter NRJ) carried out the first self-consistent numerical evolutionary calculations of brown dwarfs (in the mass range of 0.01 – $0.085 M_\odot$), through all three evolutionary phases described above, up to ages in excess of the age of the Galaxy. D'Antona and Mazzitelli (DM) have also recently calculated models of brown dwarfs with masses as small as $0.04 M_\odot$ but only for bolometric luminosities of $\sim 10^{-5} L_\odot$ or greater. To the extent that the results overlap, we find reasonable agreement between the work of NRL and that of DM. Other studies of the evolution of brown dwarfs and the interpretation of the observations of VB 8B that were recently presented at the George Mason University Workshop on Brown Dwarfs (notably those of Hubbard 1986; Lunine, Hubbard, and Marley 1986*a*; Nelson, Rappaport, and Joss 1986*a*; Stevenson 1986) show good overall agreement.

Although the theoretical cooling curves of low-mass stars are now in reasonably good agreement, there remain several large uncertainties in the input physics that must be considered when constructing models of such stars. In particular, (i) the atmospheric radiative opacities are poorly known for the temperatures of interest ($\lesssim 2500$ K), and (ii) it is difficult to evaluate the microphysics that affects the thermodynamic properties of the matter within the zones of partial ionization and molecular dissociation in the stellar envelope. In addition, there remain relatively small uncertainties in the equation of state appropriate to the stellar interior.

In this paper, we have refined the calculations carried out by NRJ and, more importantly, we have systematically explored the sensitivity of our results to some of the more important remaining uncertainties in the input physics outlined above. We also present more details of the evolution of the stellar interiors than were given by NRJ. In § II we describe our stellar models and discuss the methodology used to investigate the major uncertainties in the input physics. In § III we present the detailed results of our evolutionary calculations, with particular emphasis on the sensitivity of these results to the residual uncertainties in the input physics. In § IV we utilize our cooling curves to interpret the observations of VB 8B and to calculate brown-dwarf luminosity functions. Our conclusions are summarized in § V.

II. ASSUMPTIONS AND METHOD

The evolution of low-mass stars was carried out with a simplified stellar evolution code, similar to one which we have previously used extensively for binary stellar evolution calculations (see, e.g., RJW; Rappaport and Joss 1984; Nelson, Rappaport, and Joss 1986*b*) and for preliminary calculations of brown-dwarf evolution (NRJ). One of the main advantages in using such a code is that a systematic investigation of the sensitivity of the evolutionary sequences to various changes in the input physics can be readily carried out. The stellar evolution code has the following simplifying features: (1) The hydrostatic structure of the stellar interior is taken to be that of a modified $n = 3/2$ polytrope. (2) The photosphere is assumed to satisfy a simple pressure boundary condition, $P_s \kappa_s = 2/3g$ (where P_s , κ_s , and g are the pressure, Rosseland mean radiative opacity, and gravitational acceleration at the photosphere, respectively). (3) The specific entropy, s , in the interior is matched directly to that at the photosphere, thus bypassing the complicated physics of the stellar envelope, wherein partial ionization and molecular dissociation zones are found. A similar set of assumptions has previously been used by Hubbard (1973) to evolve models of the Jovian planets (see also Hubbard and Smoluchowski 1973). In this paper, we explore the sensitivity of our results to the use of a simple pressure boundary condition and, at the same time, we test a wide range of possible radiative opacity laws for the stellar atmosphere. We also study extensively the sensitivity of our results to the accuracy of the entropy-matching technique that our code employs.

The assumption of an $n = 3/2$ polytrope structure is a good approximation for times during the evolution when (i) the star is nearly completely convective or (ii) the electron gas in the stellar interior is substantially degenerate, or both. In fact, if one assumes uniform specific entropy, as would be the case when the entire interior was undergoing efficient convection, then an $n = 3/2$ polytropic structure is an exact representation of a star composed of a fully ionized, arbitrarily degenerate, nonrelativistic, perfect gas. We shall assume that brown dwarfs are essentially isentropic throughout their interiors, since the interiors are unstable against convection throughout most of their evolution and since the resultant convection should be highly efficient; the validity of this assumption will be examined in the next section. However, when interactions among the various constituent particles become important, the thermodynamics becomes more complicated and the stellar interior is no longer precisely described by an $n = 3/2$ polytrope. For the ranges of density and temperature of interest, the most important corrections to the thermodynamics of the stellar interior are those resulting from Coulomb interactions among the constituent particles of the plasma. The Coulomb contribution to the specific entropy is not constant throughout an $n = 3/2$ polytrope, so that modifications to the polytropic equation of state must be incorporated in order to preserve uniform specific entropy.

In our treatment of the stellar evolution, we first use the $n = 3/2$ polytropic equation of state (i.e., $P = K\rho^{5/3}$, where P and ρ are the pressure and density, respectively, and K , the polytropic constant, is invariant throughout the model) to define an approximate hydrostatic and thermal structure for each stellar model, and we then treat the Coulomb interactions as a perturbation to this structure. We rely on comparisons with completely isentropic models (with Coulomb corrections

included in the microphysics of the stellar interior) in order to obtain a realistic estimate of the magnitude of the effects of the Coulomb interactions. To this end, we constructed isentropic models covering a range of masses and values of specific entropy appropriate to the brown dwarfs under consideration. For an $n = 3/2$ polytrope composed of a nonrelativistic perfect gas, the ratio $\rho/T^{3/2}$, which is proportional to the Fermi-Dirac integral of index $\frac{1}{2}$ ($F_{1/2}$), is invariant throughout the star. However, according to our isentropic models, $\rho/T^{3/2}$ decreases with increasing distance from the stellar center, while the ratio of the absolute value of the Coulomb pressure, $|P_{\text{Coul}}|$, to the total pressure increases. Interestingly, the ratio of average density to central density for all of the isentropic models considered is given approximately by

$$\left(\frac{\bar{\rho}}{\rho_c}\right) \approx \frac{1 + 2\lambda}{5.99}, \quad \lambda \equiv \left(\frac{|P_{\text{Coul}}|}{P}\right)_c. \quad (1)$$

(We shall use the subscript c to denote parameters evaluated at the stellar center). As λ approaches zero, equation (1) reproduces the $(\bar{\rho}/\rho_c)$ relation for an $n = 3/2$ polytrope. Thus, equation (1) implies that isentropic models should be less centrally condensed than a simple $n = 3/2$ polytrope.

Our approach to calculating the stellar structure is similar to that which we have used previously when considering $n = 3/2$ polytropes (see, e.g., RJW). Using the $n = 3/2$ polytropic equation of state, with the polytropic constant evaluated at the stellar center (i.e., $K = K_c$), we solve the Lane-Emden equation. Thus K_c , M , and the inferred stellar radius, R^* , are interrelated according to $K_c = 0.424GR^*M^{1/3}$, as for an ordinary $n = 3/2$ polytrope (with no Coulomb corrections to the equation of state). However, K is not uniform throughout our isentropic models, and consequently R^* is only an approximate value for the stellar radius. Using equation (1), we find that the actual radius, R , is related to R^* according to $R \approx (1 + 2\lambda)^{-1/3}R^*$ (for a star of given mass and specific entropy and for $\lambda \ll 1$). The exact thermal structure of our models is not fully specified, but as a good approximation we take $F_{1/2}$ to be a constant throughout each model (i.e., $\rho/T^{3/2} \approx \rho_c/T_c^{3/2}$).

An evolutionary sequence of models is computed by determining the change, δs , in the specific entropy (which yields the change in K_c), so that the star evolves from one isentropic state to another. To calculate δs , we need to know the thermal structure of the model, since δs is proportional to the mass integral of the temperature profile. We have evaluated this integral for our completely isentropic models and find that

$$\tau \equiv \int T dM \approx \frac{2}{7} \frac{\mu m_u}{k} \frac{(1 + \lambda)}{D_c} \left(\frac{GM^2}{R}\right), \quad (2)$$

(see, e.g., eqs. [14]–[15] in RJW), where μ is the mean molecular weight, m_u is the atomic mass unit, k is Boltzmann's constant, and D_c is the ratio of total perfect gas pressure to ideal gas pressure, evaluated at the stellar center. (This result also holds exactly for an $n = 3/2$ polytrope composed of a perfect [$\lambda = 0$], nonrelativistic gas). Once the surface boundary conditions are determined for a particular model in an evolutionary sequence, the value of δs can be obtained from the equation $\delta s = (L_{\text{nuc}} - L)\tau^{-1}\delta t$, where L_{nuc} and L are the nuclear and bolometric luminosities, respectively, and δt is the time step between models. Thus, a new value of K_c can be deduced that in turn allows the other properties of the new model to be computed. Through the implementation of this scheme, we have more accurately simulated the properties of low-mass

stars by including Coulomb corrections to the equation of state (cf. RJW) as well as satisfied, to a high degree of accuracy, the first law of thermodynamics and the virial theorem.

The equation of state for the interiors of our models describes a completely ionized, nondegenerate gas of nuclei undergoing Coulomb interactions immersed in a uniform (unpolarized), arbitrarily degenerate, perfect gas of electrons. We calculated the Coulomb contribution, F_{Coul} , to the Helmholtz free energy of the plasma as a function of the plasma parameter Γ (the ratio of nearest neighbor Coulomb energy to thermal kinetic energy per nucleus) from the appropriate Coulomb correction, U_{Coul} , to the internal energy. We evaluated the normalized Coulomb correction, F_{Coul}/NkT , to the free energy from the expression $F_{\text{Coul}}/NkT = \int_0^1 \mathcal{U}(\Gamma)\Gamma^{-1}d\Gamma$, where $\mathcal{U} \equiv U_{\text{Coul}}/NkT$. The total contribution to U_{Coul} from each ionic species of the multicomponent plasma was calculated according to the method suggested by Ichimaru (1982). To ensure a high level of accuracy over a wide range of Γ , we determined U_{Coul} in three separate domains of Γ . In the limit of a weakly coupled plasma ($\Gamma \leq 0.1$), we adopted the Abe cluster expansion formula given by Hansen (1973). For $0.1 \leq \Gamma \leq 1$, we devised a fitting formula wherein $U_{\text{Coul}}(\Gamma)$ was fitted to values of the hypernetted chain (HNC) approximation (see Slattery, Doolen, and DeWitt 1980) for values of Γ between 0.1 and 0.6, and to the Monte Carlo results of Slattery, Doolen, and DeWitt (1982) for Γ between 0.6 and 1. The resultant fit to $U_{\text{Coul}}(\Gamma)$ agrees with published values to within $\sim 1\%$ and was designed so that the fitted values of $U_{\text{Coul}}(\Gamma = 0.1)$ and $U_{\text{Coul}}(\Gamma = 1)$ agreed with the Abe expansion and Monte Carlo results, respectively. For the case of a strongly coupled plasma ($\Gamma \geq 1$), we used the fitting formula for U_{Coul} published by Slattery, Doolen, and DeWitt (1982). Once F_{Coul} was calculated from our expression for U_{Coul} , the Coulomb corrections to the pressure and specific entropy were easily calculated by application of standard thermodynamic relations. According to our fitting formula for F_{Coul} , we find that F_{Coul}/NkT at $\Gamma = 1$ is equal to -0.4385 ; Slattery, Doolen, and DeWitt (1982) obtain a more precise value of -0.4363 . This difference implies an error in our expression for the specific entropy of ~ 0.002 (in units of k/m_u) for the strongly coupled regime. This error is negligible compared to the uncertainties in entropy matching within our stellar models (see § III).

Other contributions to the equation of state from quantum ion phenomena and electronic terms (e.g., electron exchange) are less important in the range of temperatures and densities pertinent to the degenerate cooling phase of the evolution of our stellar models (see § III) and have not been included in our calculations. For example, we find that the Helmholtz free energy associated with the first-order correction for quantum ion effects (in the Wigner expansion) is $\sim 1\%$ of $|F_{\text{Coul}}|$ throughout the range of ρ and T relevant to our calculations. Of the electronic terms, the electron exchange correction to the pressure is the largest (in the high-density, low-temperature regime), but its magnitude is still less than $\sim 50\%$ that of the Coulomb correction. We also did not include thermodynamic effects associated with the Coulomb lattice state, since hydrogen and helium do not freeze in any of our models (the phase transition to a lattice occurs for $\Gamma \approx 178$).

As mentioned above, the total specific entropy in the interior was matched directly to the specific entropy at the photosphere. The equation of state at the photosphere is taken to be that of a perfect, nondegenerate gas and takes into account the partial association of hydrogen into molecular form. The effect

of excitation of rotational and vibrational states of H_2 on the specific entropy at the photosphere was calculated by use of a table of energy levels from Bishop and Shih (1976). Atmospheric radiative opacities were taken from a fitting formula to the Alexander opacities (Alexander 1975; RJW). For low temperatures ($\lesssim 2500$ K), the atmospheric radiative opacities become difficult to estimate accurately because of the contribution from molecules and the possible formation of grains (see, e.g., Alexander 1975; Alexander, Johnson, and Rypma 1983). We therefore chose to simply parameterize the opacity coefficients at low temperatures by setting κ equal to a limiting value, κ_{\min} , whenever the value of κ given by fitting formula "A" of RJW to the Alexander (1975) opacities fell below κ_{\min} . The value of κ_{\min} was varied from one model to another; in our standard models, we set $\log(\kappa_{\min}/\text{cm}^2 \text{g}^{-1}) = -1.5$.

We assumed a solar composition ($X = 0.7$, $Z = 0.02$) plus a primordial abundance of deuterium of 5×10^{-5} by mass (Gautier and Owen 1982). Nuclear burning, including weak and strong screening corrections, were incorporated as described by RJW and Rappaport, Verbunt, and Joss (1983). In the present calculations, the He^3 -burning portion of the p - p chain was excluded in calculating the nuclear energy generation rate because of the breakdown of nuclear quasi-equilibrium, which was, in turn, a result of the low internal temperatures of these low-mass stars.

Much of the uncertainty in the evolution due to the possible existence of nonadiabatic (superadiabatic and radiative) zones in the stellar envelope can be incorporated into a single parameter, namely, the difference, $\Delta s \equiv s_s - s_i$, in specific entropy between the stellar interior (with specific entropy s_i) and that at the photosphere (specific entropy s_s). Such a formulation can also take into account many of the other uncertainties in the microphysics of the stellar envelope and stellar interior, as well as any small inaccuracies introduced by our use of a modified $n = 3/2$ polytrope. We have chosen three algorithms for mismatching the entropy in addition to our standard model with $\Delta s = 0$: (i) $\Delta s = +1$; (ii) $s_s = 5/4s_i$; and (iii) $\Delta s = -1$ (where we have expressed specific entropy in units of k/m_u). We consider this range of entropy mismatches to be fairly encompassing, based on (i) our analysis of recently calculated low-temperature, flux-corrected model atmospheres (Auman 1969; Mould 1976), which indicate that Δs is never greater than ~ 0.5 for stars of the appropriate surface gravity ($\log g \gtrsim 3.5$), (ii) our own unpublished Henyey-type evolutionary calculations of stars at low effective temperatures ($1600 \lesssim T_e \lesssim 2500$ K), (iii) the fact that s_i varies only from 16 to 6 throughout the course of the evolution in any of our standard models (covering a range of nearly a factor of 10^4 in central density), and (iv) our estimate that any further changes to s_i resulting from additional corrections to the equation of state should be no larger in absolute value than the correction due to Coulomb interactions (which yields changes in s_i of less than 0.7).

In order to simulate the uncertainties in the atmospheric radiative opacities due to the formation of grains and molecules at low temperatures, we computed evolutionary sequences for a range of values of κ_{\min} with $\log(\kappa_{\min}/\text{cm}^2 \text{g}^{-1}) = -1.0, -1.5, -2.5$, and -3.5 , as well as a sequence in which fitting formula "A" of RJW was extrapolated to arbitrarily low effective temperatures. We take $\log \kappa_{\min} = -3.5$ to be a reasonable lower bound on κ_{\min} based on the work of Stahler, Palla, and Salpeter (1986), who derived low-temperature ($\gtrsim 1000$ K) Rosseland mean opacities for zero-metal compositions. The wide range of values of κ_{\min} that we

have considered also simulates the uncertainty arising from our choice of the numerical coefficient $2/3$ that is used in our approximate pressure boundary condition.

III. RESULTS

We carried out evolutionary calculations for masses in the range of 0.01 – $0.10 M_\odot$. The evolution of R for our standard models with $M = 0.01, 0.02, 0.04, 0.06$, and $0.08 M_\odot$ is shown in Figure 1. The models all started with an initial radius of $\sim 1 R_\odot$, a value very large compared to the star's ultimate radius at late ages. For early ages, the stellar radius contracts with elapsed time, t , approximately as $t^{-1/3}$, as can be demonstrated analytically if one assumes a completely convective model for which the effective temperature remains approximately constant (see, e.g., Hayashi and Nakano 1963). We note that for very early ages ($t < 10^6$ yr), the evolution is highly uncertain because of the possible effects of rapid stellar rotation and mass loss or accretion (see, e.g., Gehrz, Black, and Solomon 1984). Furthermore, at these early ages, the material in the stellar interior may not be fully ionized as we have assumed. For ages near 10^6 yr, there is an interval on each evolutionary curve (for $M \gtrsim 0.015 M_\odot$), where R remains nearly constant; this corresponds to the deuterium-burning main-sequence phase (see, also, Bodenheimer 1966 and GHG). After deuterium exhaustion the star contracts, and for a period of time the internal temperatures increase (in accordance with the virial theorem). For stars with masses in excess of $\sim 0.08 M_\odot$ the internal temperatures reach sufficiently high values to establish thermal equilibrium through thermonuclear burning via the p - p chain (which essentially terminates at He^3 for the low internal temperatures of interest here). For lower mass stars, thermal equilibrium is never achieved, and the internal temperatures ultimately decline as electron degeneracy increasingly provides the bulk of the pressure support for the star. These low-mass stars are thus destined to cool forever toward a completely degenerate configuration. The mass-radius relation of a fully degenerate star supported solely by the pressure of a perfect electron gas is given by $R \propto M^{-1/3}$; however, when a more realistic equation of state is used (see, e.g., Zapolsky and Salpeter 1969), then R is approximately proportional to $M^{-1/6}$ for zero-temperature stars in the mass range of interest.

The evolution of the effective temperature for our standard models is presented in Figure 2. The temperatures during the contraction phase remain relatively constant (see, e.g., Hayashi and Nakano 1963) and then decline after much of the available gravitational energy has been exhausted. Since all stars with masses in the range of 0.01 – $0.08 M_\odot$ eventually attain a similar radius (to within $\pm 20\%$), the higher mass stars, which initially have a larger store of gravitational potential energy ($\propto M^2$), require significantly longer times to cool to the same effective temperature. For late ages ($5 \times 10^8 \text{ yr} \lesssim t \lesssim 2 \times 10^{10} \text{ yr}$) the effective temperatures of stars with masses in the range of ~ 0.01 – $0.06 M_\odot$ are given approximately by

$$T_e \simeq 1270 \left(\frac{M}{0.05 M_\odot} \right)^{0.68} \left(\frac{t}{10^9 \text{ yr}} \right)^{-0.29} \text{ K}, \quad (3)$$

where the rms error in the fit is $\sim 3\%$ of T_e . We caution that this fitting formula should not be extrapolated to much earlier ages, or to much larger masses ($M \gtrsim 0.07 M_\odot$).

The results shown in Figures 1 and 2 can be combined to yield the evolution of the stellar luminosity, L , in our standard

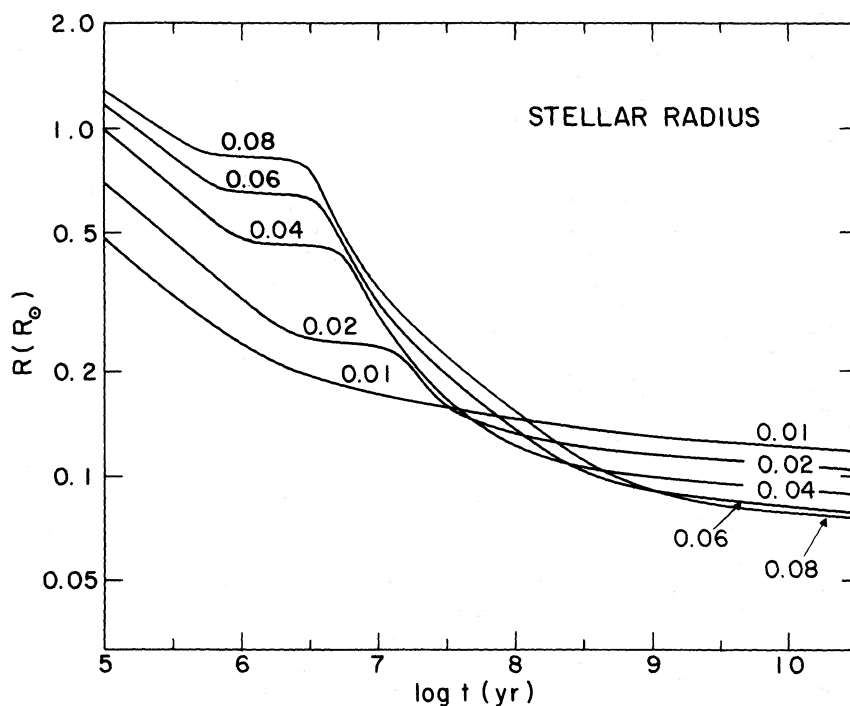


FIG. 1.—Evolution of the stellar radius, R , as a function of age, t , for the standard models of very low mass stars with masses in the range of 0.01 – $0.10 M_{\odot}$. Each track is labeled with the corresponding stellar mass in units of solar masses. The plateau regions evident near $t = 10^6$ – 10^7 yr are due to the burning of a small quantity (5×10^{-5} by mass) of primordial deuterium.

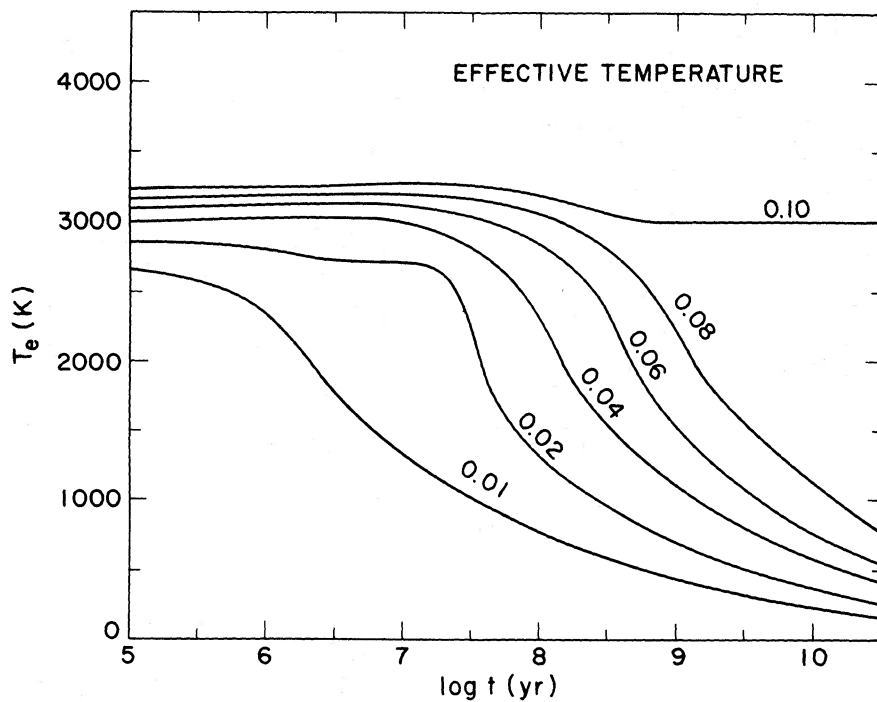


FIG. 2.—Evolution of the effective temperature, T_e as a function of age t , for the standard models of very low mass stars with masses in the range of 0.01 – $0.10 M_{\odot}$. Each track is labeled with the corresponding stellar mass in units of solar masses. Stars with masses in excess of $\sim 0.08 M_{\odot}$ ultimately achieve thermal equilibrium through hydrogen burning (i.e., they attain hydrogen-burning main-sequence status). Stars of lower mass cool indefinitely toward a completely degenerate configuration. For $T_e \lesssim 1000$ K the displayed cooling curves become increasingly uncertain.

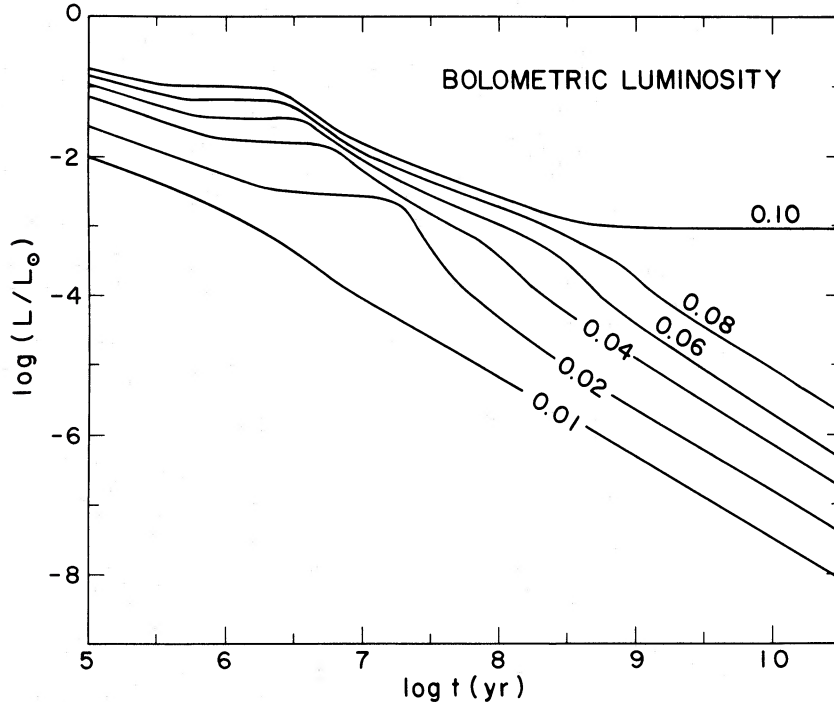


FIG. 3.—Evolution of the bolometric luminosity, L , as a function of age, t , for the standard models of very low mass stars with masses in the range of 0.01 – $0.10 M_{\odot}$. Each track is labeled with the corresponding stellar mass in units of solar masses.

models (see Fig. 3). For late ages, L is given approximately by

$$L \approx 2.1 \times 10^{-5} \left(\frac{M}{0.05 M_{\odot}} \right)^{2.34} \left(\frac{t}{10^9 \text{ yr}} \right)^{-1.22} L_{\odot}. \quad (4)$$

The largest error in this equation results from the relatively poor fit of the factor involving M . Nonetheless, the rms error between the actual value of L in the standard models and the values given by equation (4) is only $\sim 10\%$ of L . Equations (3) and (4) are in good agreement with the results of earlier work by Stevenson (1978) and with the results of other more recent calculations (see, e.g., Stevenson 1986).

Some of the numerical results from our standard models are given in Table 1. In addition to the evolution of the stellar parameters shown in Figures 1–3, we include in Table 1 the evolution of ρ_c , T_c , an electron degeneracy parameter, D_c , the parameter $\lambda \equiv (|P_{\text{Coul}}|/P)_c$, and the ratio of nuclear to bolometric luminosity (L_{nuc}/L).

As discussed in § II, we also carried out a series of evolutionary runs designed to test the sensitivity of our models to the assumption that the specific entropy in the stellar interior is equal to that at the photosphere. The evolution of T_e for a $0.06 M_{\odot}$ star with various degrees of entropy mismatch (see § II for details) is shown in Figure 4. Note that early in the evolution of the models with $\Delta s > 0$, the effective temperatures are higher than for the model with $\Delta s < 0$. At later ages the reverse of this condition obtains. This reversal of temperatures is a simple consequence of the virial theorem and the fact that the total energy to be extracted from the stellar contraction is nearly fixed. For $t < 2 \times 10^9$ yr, the uncertainty in T_e at any given age (defined as the half width between extreme model values) is less than $\sim 15\%$. For $t > 2 \times 10^9$ yr the uncertainty in T_e remains fairly constant at ~ 120 K. The corresponding uncertainty in the time required for a star of mass $0.06 M_{\odot}$ to

cool to a given temperature is less than a factor of 2 for $t \gtrsim 3 \times 10^8$ yr and for all tested variations of entropy mismatch. A similar series of tests, involving entropy mismatches in a model with $M = 0.02 M_{\odot}$, is shown in Figure 5. In this case the uncertainty in T_e is always less than 15%, and for $t > 10^8$ yr the uncertainty is only ~ 50 K. The uncertainty in cooling times for this case is less than a factor of 1.6.

Evolutionary tracks for our 0.02 and $0.06 M_{\odot}$ models in the central-density/central-temperature ($\rho_c - T_c$) plane are shown in Figure 6. For each stellar mass, the evolutionary track is marked with different values of the entropy mismatch. The track is labeled where the evolution of a particular model sequence has reached ages of 10 and 20 billion years. Note that once M and ρ_c are specified in our models, T_c is uniquely defined; hence, for a given mass, there is only a single track in the $\rho_c - T_c$ plane. However, the surface boundary conditions determine the time required to reach any given point along an evolutionary track. Also indicated in the figure are several contours of constant electron degeneracy (as determined by the value of $F_{1/2}$ at the stellar center), as well as contours of constant Γ_c (the plasma parameter evaluated at the stellar center). We find that the internal temperatures at late ages vary significantly (by a factor of ~ 4) over the range of assumed entropy mismatches. We also note that the largest value of Γ_c encountered at the stellar center is ~ 15 . Thus, although the values of Γ will increase somewhat with increasing distance from the stellar center, the models we have considered will not undergo crystallization into a Coulomb lattice over any significant fraction of their volumes for ages up to the age of the Galaxy. Moreover, Debye cooling should be unimportant in these low-mass stars (cf. Tarter 1975).

The sensitivity of our models to uncertainties in the atmospheric radiative opacities is shown in Figures 7, 8, and 9. The evolution of T_e for a star with $M = 0.06 M_{\odot}$ and for a wide

TABLE 1
EVOLUTIONARY PROPERTIES OF LOW-MASS STARS^a

log (t/yr)	R/R_{\odot}	$T_{\text{e}}(K)$	log (L/L_{\odot})	ρ_{c}	T_{c}	D_{c}	λ	log (L_{nucl}/L)
$M = 0.01 M_{\odot}$								
6.0.....	0.241	2334	-2.82	4.6	0.25	1.34	0.160	-5.65
6.2.....	0.217	2137	-3.06	6.2	0.26	1.43	0.162	-4.90
6.4.....	0.201	1898	-3.34	7.9	0.26	1.52	0.164	-4.33
6.6.....	0.188	1676	-3.60	9.5	0.26	1.62	0.165	-3.90
6.8.....	0.179	1491	-3.85	11.0	0.26	1.71	0.167	-3.59
7.0.....	0.171	1334	-4.08	12.5	0.26	1.82	0.168	-3.36
7.2.....	0.165	1196	-4.31	14.1	0.25	1.93	0.170	-3.19
7.4.....	0.159	1073	-4.53	15.6	0.25	2.06	0.171	-3.08
7.6.....	0.154	963	-4.75	17.2	0.24	2.20	0.173	-3.03
7.8.....	0.149	862	-4.96	18.8	0.23	2.36	0.174	-3.02
8.0.....	0.145	774	-5.17	20.4	0.22	2.55	0.176	-3.08
8.2.....	0.141	689	-5.40	22.1	0.21	2.76	0.178	-3.17
8.4.....	0.138	612	-5.63	23.7	0.20	3.01	0.180	-3.32
8.6.....	0.135	543	-5.85	25.3	0.18	3.28	0.181	-3.51
8.8.....	0.132	481	-6.08	26.8	0.17	3.60	0.183	-3.74
9.0.....	0.130	425	-6.31	28.3	0.16	3.95	0.185	-4.01
9.2.....	0.127	375	-6.55	29.7	0.15	4.35	0.187	-4.31
9.4.....	0.125	330	-6.78	31.1	0.13	4.81	0.189	-4.64
9.6.....	0.123	291	-7.01	32.4	0.12	5.32	0.190	-5.00
9.8.....	0.122	255	-7.25	33.6	0.11	5.89	0.192	-5.37
10.0.....	0.120	224	-7.49	34.8	0.10	6.53	0.193	-5.76
10.2.....	0.119	196	-7.73	36.0	0.09	7.25	0.195	-6.16
10.4.....	0.118	172	-7.96	37.1	0.09	8.05	0.196	-6.57
$M = 0.02 M_{\odot}$								
6.0.....	0.321	2785	-2.26	4.3	0.43	1.15	0.091	-2.13
6.2.....	0.279	2749	-2.40	6.5	0.47	1.19	0.091	-1.08
6.4.....	0.250	2708	-2.52	9.1	0.51	1.24	0.092	-0.32
6.6.....	0.239	2687	-2.58	10.4	0.52	1.26	0.092	-0.05
6.8.....	0.236	2679	-2.60	10.9	0.53	1.27	0.093	-0.02
7.0.....	0.231	2669	-2.62	11.5	0.53	1.28	0.093	-0.03
7.2.....	0.221	2642	-2.68	13.2	0.54	1.31	0.093	-0.06
7.4.....	0.186	2494	-2.93	22.0	0.58	1.45	0.095	-0.60
7.6.....	0.150	1844	-3.64	41.8	0.58	1.82	0.099	-9.20
7.8.....	0.139	1491	-4.07	52.4	0.55	2.07	0.101	-8.87
8.0.....	0.132	1271	-4.39	60.3	0.52	2.29	0.103	-8.73
8.2.....	0.127	1106	-4.67	67.3	0.49	2.53	0.105	-8.69
8.4.....	0.124	967	-4.93	73.7	0.46	2.78	0.106	-8.69
8.6.....	0.120	851	-5.17	79.5	0.43	3.06	0.108	-8.74
8.8.....	0.118	750	-5.41	85.1	0.40	3.37	0.109	-8.83
9.0.....	0.115	661	-5.65	90.3	0.37	3.73	0.111	-8.95
9.2.....	0.113	582	-5.89	95.4	0.34	4.12	0.112	-9.10
9.4.....	0.111	512	-6.12	100.2	0.31	4.57	0.113	-9.27
9.6.....	0.109	450	-6.36	104.8	0.28	5.09	0.115	-9.47
9.8.....	0.108	395	-6.60	109.1	0.26	5.66	0.116	-9.69
10.0.....	0.106	346	-6.84	113.3	0.24	6.32	0.117	-9.92
10.2.....	0.105	303	-7.08	117.2	0.21	7.05	0.119	-10.16
10.4.....	0.104	265	-7.32	121.0	0.19	7.88	0.120	-10.41
$M = 0.04 M_{\odot}$								
6.0.....	0.477	3016	-1.78	2.8	0.61	1.06	0.051	-0.25
6.2.....	0.461	3016	-1.81	3.1	0.63	1.06	0.051	-0.02
6.4.....	0.456	3016	-1.82	3.2	0.64	1.06	0.051	-0.02
6.6.....	0.445	3015	-1.84	3.5	0.65	1.06	0.051	-0.03
6.8.....	0.417	3013	-1.90	4.2	0.69	1.07	0.051	-0.09
7.0.....	0.288	2982	-2.24	12.8	0.95	1.13	0.052	-8.58
7.2.....	0.218	2919	-2.51	29.3	1.16	1.22	0.053	-6.97
7.4.....	0.179	2833	-2.74	52.7	1.30	1.33	0.054	-5.98
7.6.....	0.153	2713	-2.95	84.4	1.37	1.48	0.055	-5.29
7.8.....	0.134	2548	-3.17	124.6	1.37	1.68	0.057	-4.83
8.0.....	0.121	2245	-3.48	169.1	1.31	1.95	0.058	-4.52
8.2.....	0.114	1879	-3.85	205.3	1.23	2.22	0.060	-4.28
8.4.....	0.109	1612	-4.15	234.1	1.15	2.48	0.061	-4.16
8.6.....	0.105	1392	-4.44	259.7	1.07	2.77	0.062	-4.10
8.8.....	0.102	1217	-4.69	282.0	0.99	3.07	0.063	-4.09
9.0.....	0.100	1068	-4.94	302.7	0.92	3.41	0.065	-4.11
9.2.....	0.097	938	-5.19	322.1	0.84	3.79	0.066	-4.17
9.4.....	0.096	824	-5.43	340.4	0.77	4.22	0.067	-4.25
9.6.....	0.094	724	-5.67	357.8	0.70	4.71	0.068	-4.36
9.8.....	0.092	635	-5.91	374.3	0.64	5.27	0.069	-4.49
10.0.....	0.091	556	-6.15	389.9	0.58	5.91	0.070	-4.64
10.2.....	0.090	486	-6.39	404.8	0.52	6.64	0.071	-4.80
10.4.....	0.089	425	-6.64	418.8	0.47	7.46	0.072	-4.98

TABLE 1—Continued

log (t/yr)	R/R_{\odot}	$T_{\text{e}}(\text{K})$	$\log (L/L_{\odot})$	ρ_{c}	T_{c}	D_{c}	λ	$\log (L_{\text{nuc}}/L)$
$M = 0.06 M_{\odot}$								
6.0.....	0.653	3118	-1.45	1.7	0.69	1.03	0.036	-0.03
6.2.....	0.645	3119	-1.46	1.8	0.70	1.03	0.036	-0.02
6.4.....	0.632	3119	-1.48	1.9	0.71	1.03	0.036	-0.03
6.6.....	0.597	3121	-1.52	2.2	0.75	1.03	0.036	-0.08
6.8.....	0.422	3124	-1.82	6.3	1.04	1.06	0.036	-8.78
7.0.....	0.312	3112	-2.09	15.4	1.35	1.10	0.036	-6.92
7.2.....	0.252	3089	-2.29	29.5	1.61	1.14	0.037	-5.69
7.4.....	0.210	3054	-2.47	50.8	1.85	1.19	0.037	-4.73
7.6.....	0.178	3004	-2.64	82.6	2.05	1.26	0.038	-3.94
7.8.....	0.154	2932	-2.81	129.0	2.20	1.36	0.039	-3.28
8.0.....	0.134	2829	-2.99	193.6	2.29	1.50	0.040	-2.76
8.2.....	0.119	2680	-3.19	279.0	2.28	1.71	0.041	-2.38
8.4.....	0.107	2483	-3.42	382.3	2.16	2.01	0.042	-2.16
8.6.....	0.099	2070	-3.80	479.1	1.97	2.38	0.044	-1.95
8.8.....	0.094	1729	-4.15	552.3	1.79	2.74	0.045	-1.83
9.0.....	0.091	1482	-4.45	608.5	1.64	3.10	0.046	-1.78
9.2.....	0.089	1286	-4.72	657.0	1.50	3.48	0.047	-1.77
9.4.....	0.087	1121	-4.98	701.0	1.37	3.91	0.048	-1.80
9.6.....	0.085	979	-5.23	741.7	1.24	4.39	0.049	-1.85
9.8.....	0.084	856	-5.48	779.7	1.12	4.94	0.050	-1.93
10.0.....	0.083	748	-5.72	815.4	1.01	5.56	0.051	-2.02
10.2.....	0.081	654	-5.97	849.1	0.91	6.27	0.052	-2.14
10.4.....	0.080	570	-6.22	880.7	0.82	7.08	0.053	-2.27
$M = 0.08 M_{\odot}$								
6.0.....	0.824	3185	-1.21	1.1	0.73	1.02	0.028	-0.02
6.2.....	0.811	3186	-1.22	1.2	0.74	1.02	0.028	-0.02
6.4.....	0.783	3188	-1.25	1.3	0.77	1.02	0.028	-0.04
6.6.....	0.646	3195	-1.41	2.4	0.93	1.03	0.028	-1.41
6.8.....	0.443	3203	-1.74	7.3	1.32	1.05	0.028	-7.60
7.0.....	0.348	3201	-1.95	15.1	1.65	1.07	0.028	-6.15
7.2.....	0.286	3191	-2.13	27.3	1.96	1.10	0.028	-5.03
7.4.....	0.240	3174	-2.29	46.3	2.27	1.13	0.029	-4.10
7.6.....	0.204	3147	-2.44	75.4	2.57	1.17	0.029	-3.28
7.8.....	0.175	3108	-2.60	119.5	2.85	1.23	0.029	-2.57
8.0.....	0.151	3053	-2.76	184.7	3.09	1.32	0.030	-1.94
8.2.....	0.132	2974	-2.92	278.2	3.26	1.43	0.031	-1.41
8.4.....	0.116	2862	-3.10	403.1	3.32	1.59	0.032	-0.99
8.6.....	0.105	2716	-3.28	551.7	3.24	1.81	0.033	-0.71
8.8.....	0.096	2539	-3.47	714.8	3.04	2.11	0.034	-0.57
9.0.....	0.090	2222	-3.76	876.8	2.75	2.50	0.035	-0.46
9.2.....	0.086	1885	-4.08	992.4	2.50	2.87	0.036	-0.35
9.4.....	0.083	1649	-4.34	1076.9	2.30	3.20	0.037	-0.30
9.6.....	0.082	1457	-4.58	1150.5	2.12	3.56	0.038	-0.28
9.8.....	0.080	1286	-4.81	1219.9	1.95	3.96	0.039	-0.28
10.0.....	0.079	1127	-5.05	1288.7	1.77	4.44	0.039	-0.31
10.2.....	0.077	978	-5.32	1358.1	1.59	5.04	0.040	-0.36
10.4.....	0.076	840	-5.60	1427.7	1.41	5.78	0.041	-0.44

NOTE.— ρ_{c} = central density in units of g cm^{-3} ; T_{c} = central temperature in units of 10^6 K ; D_{c} = degeneracy parameter (ratio of total perfect gas pressure to ideal gas pressure, evaluated at the stellar center); λ = ratio of Coulomb pressure to total gas pressure, evaluated at the stellar center.

^a Standard models. The results are increasingly uncertain for $T_{\text{c}} \lesssim 1000 \text{ K}$.

range of opacity laws is shown in Figure 7. As described in § II, the opacity coefficients were taken from fitting formula "A" of RJW but with various lower limits, κ_{min} , imposed. We studied the effects on the evolution of different κ_{min} over a range of nearly four orders of magnitude. We find that for a star of mass $0.06 M_{\odot}$, this wide range of minimum opacity coefficients yields uncertainties in the effective temperatures of only $\sim 12\%$ or less for all stellar ages. The corresponding uncertainty in the cooling times is a factor of ~ 1.5 . The sensitivity to variations in κ_{min} for a $0.02 M_{\odot}$ stellar model is shown in Figure 8. The uncertainties in effective temperature at a given age are again less than $\sim 12\%$, and the corresponding uncertainties in the cooling times are also similar to those for the $0.06 M_{\odot}$ model.

Evolutionary tracks in the $\rho_{\text{c}} - T_{\text{c}}$ plane for the $0.02 M_{\odot}$ and $0.06 M_{\odot}$ models, with various values of κ_{min} , are shown in Figure 9. The two sets of points on each of the evolutionary tracks indicate the evolutionary state of a model at ages of 10 and 20 billion years, respectively. The largest value of Γ_{c} for any of these models is ~ 30 . However, the values of κ_{min} corresponding to the largest values of Γ_{c} are becoming unrealistic. More plausible values of κ_{min} ($\sim 10^{-2} \text{ cm}^2 \text{ g}^{-1}$) yield maximum central values of $\Gamma_{\text{c}} \approx 10$. Thus, as in our study of possible entropy mismatches, we find that crystallization and Debye cooling will be unimportant for nearly any plausible low-temperature opacity law.

We have also tested the sensitivity of our models to the

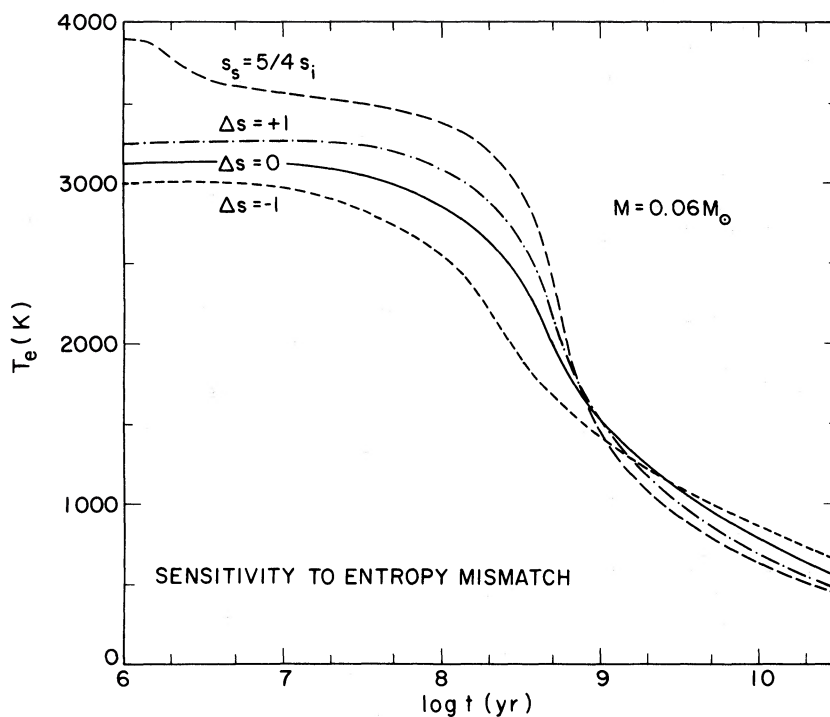


FIG. 4.—Sensitivity of the cooling of a $0.06 M_{\odot}$ stellar model to various mismatches in the specific entropy between the stellar interior and stellar surface. Each track is labeled according to the algorithm by which specific entropy is mismatched (*see text*).

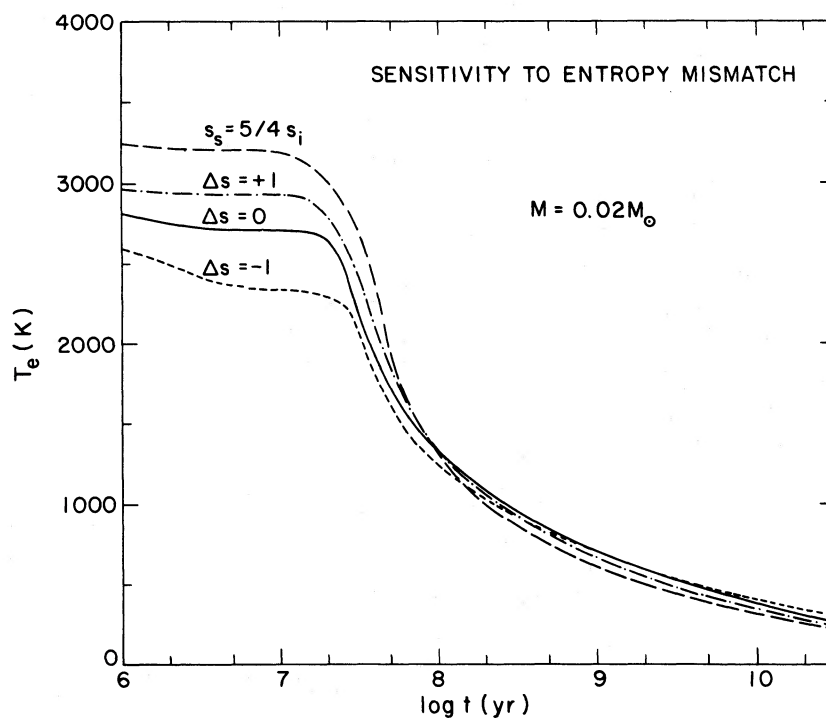


FIG. 5.—Sensitivity of the cooling of a $0.02 M_{\odot}$ stellar model to various mismatches in the specific entropy between the stellar interior and stellar surface. Each track is labeled according to the algorithm by which specific entropy is mismatched (*see text*).

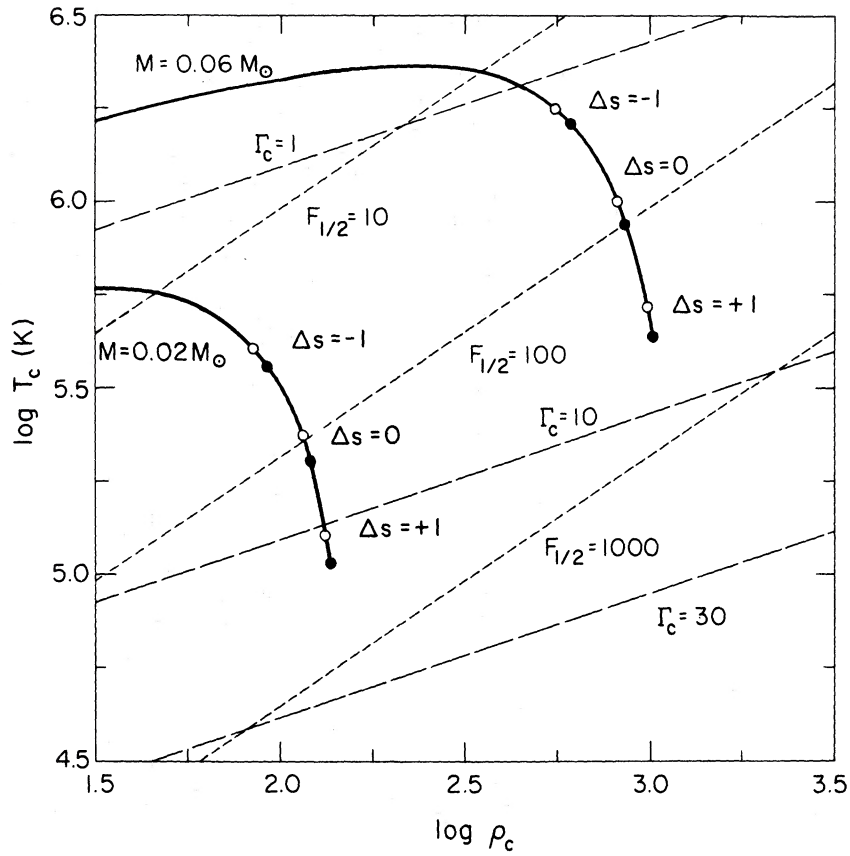


FIG. 6.—Sensitivity of the central density, ρ_c , and central temperature, T_c , of $0.02 M_\odot$ and $0.06 M_\odot$ stellar models to various mismatches in specific entropy between the stellar interior and stellar surface (see text for details). Each open circle on the two curves denotes the internal properties of a particular model at an age of 10^{10} yr; the filled circles correspond to an age of 2×10^{10} yr. $F_{1/2}$ and Γ_c are the Fermi-Dirac integral of index $1/2$ and the mean plasma parameter (each evaluated at the stellar center), respectively.

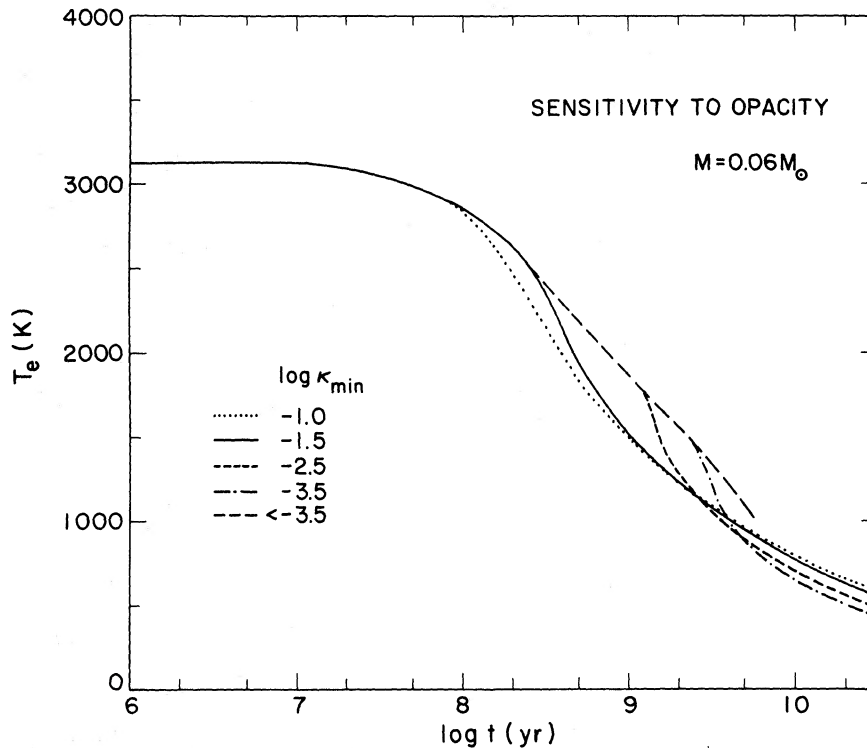


FIG. 7.—Sensitivity of the cooling of a $0.06 M_\odot$ stellar model to various assumed minimum values for the atmospheric radiative opacity coefficient, κ_{\min} (expressed in units of $\text{cm}^2 \text{g}^{-1}$). The label $\log \kappa_{\min} < -3.5$ refers to the fully extrapolated Alexander opacity law without grains (see text).

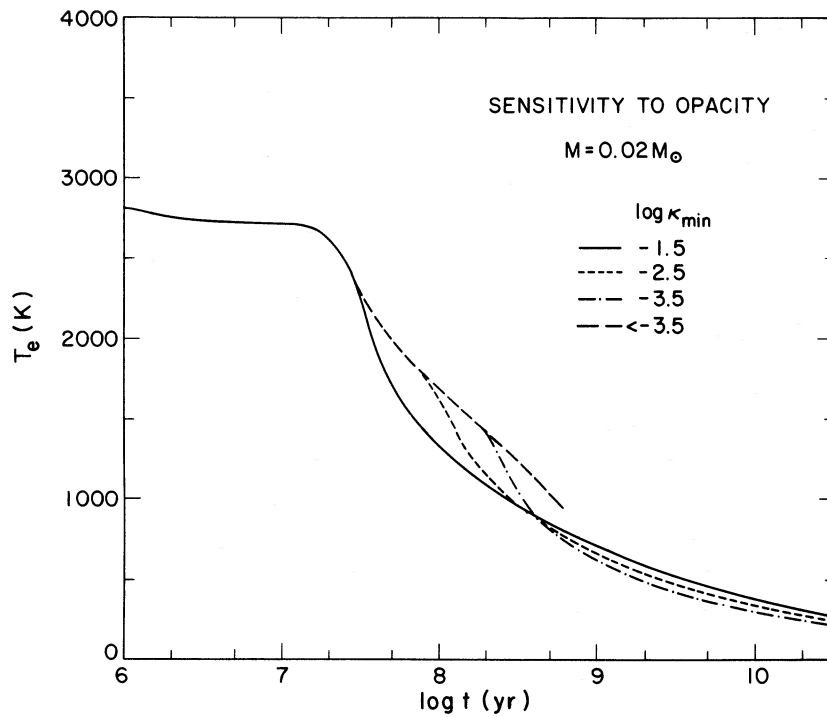


FIG. 8.—Sensitivity of the cooling of a $0.02 M_{\odot}$ stellar model to various assumed minimum values for the atmospheric radiative opacity coefficient, κ_{\min} (expressed in units of $\text{cm}^2 \text{g}^{-1}$). The label $\log \kappa_{\min} < -3.5$ refers to the fully extrapolated Alexander opacity law without grains (*see text*).

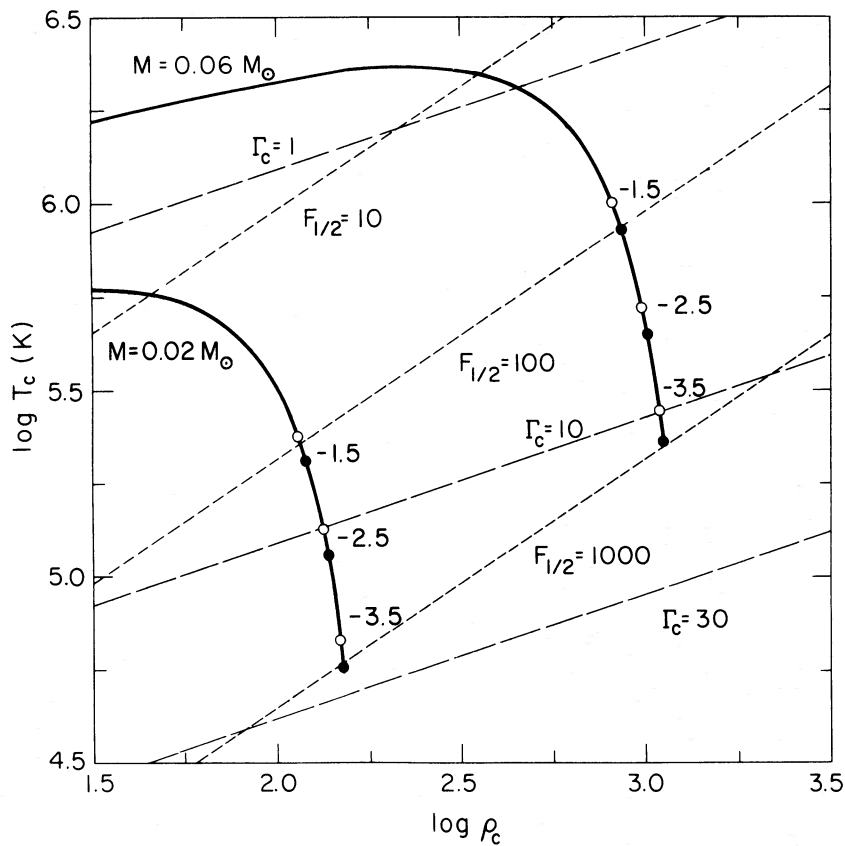


FIG. 9.—Sensitivity of the central density, ρ_c , and central temperature, T_c , of $0.02 M_{\odot}$ and $0.06 M_{\odot}$ stellar models to various assumed minimum values for the atmospheric radiative opacity coefficient, κ_{\min} . Each open circle on the two curves denotes the internal properties of a particular model [denoted by the value of $\log(\kappa_{\min}/\text{cm}^2 \text{g}^{-1})$] at an age of 10^{10} yr; the filled circles correspond to an age of 2×10^{10} yr. $F_{1/2}$ and Γ_c are the Fermi-Dirac integral of index 1/2 and the mean plasma parameter (each evaluated at the stellar center), respectively.

assumed equation of state for the stellar interior. In particular, we evaluated the effects of the Coulomb corrections to the equation of state and also simulated the inclusion of non-Coulombic terms (e.g., electron exchange effects). To do this, we arbitrarily varied the value of λ , the parameterized correction to the perfect-gas equation of state (see § II), from 0.5 to 1.5 times its actual value. We found that, at a given age, ρ_c and T_c can vary by factors of up to ~ 2 , depending on the assumed value of λ . However, for $M \lesssim 0.06 M_\odot$, the evolution of the observed stellar parameters (T_e and L) is fairly insensitive to variations of the equation of state in this range.

Although, as discussed above, the cooling tracks of stars with masses $\sim 0.06 M_\odot$ or smaller are not very sensitive to changes in the input physics, we find that the minimum mass required for a star to attain thermal equilibrium via hydrogen burning (i.e., to achieve main-sequence status) is quite sensitive to the assumed surface boundary conditions, the equation of state in the interior and, as noted in § I (see Rappaport and Joss 1984), the chemical composition. For example, we find that for plausible changes in the surface boundary conditions and equation of state, a star of only $\sim 0.075 M_\odot$ can achieve main-sequence status. We also find that there can be a prolonged interval during which a star with a mass slightly less than the minimum main-sequence mass can hover near thermal equilibrium, and that such a star will require a time comparable to the age of the Galaxy to cool below the temperature of VB 8B (see also NRJ and DM). This type of behavior is independent of the exact value of the minimum main-sequence mass. We are currently carrying out a more detailed investigation of the sensitivity of the properties of stars near the end of the main sequence to the assumed input physics, and we shall report on the results of this study elsewhere (Nelson, Rappaport, and Joss 1986c).

Finally, as a self-consistency check, we monitored the interior of our models for convective instability. Conductive opacities for the stellar interior were taken from fitting formulae derived by Iben (1975) based on the conductive opacity calculations by Hubbard and Lampe (1969). The results of our checks indicate that all of our models should be completely convective for $t \lesssim 10^9$ yr, and models with $M \lesssim 0.02 M_\odot$ are completely convective for ages up to 10^{10} yr. In particular, for an age equal to that of the solar system ($\sim 4.5 \times 10^9$ yr), stars with $M \lesssim 0.03 M_\odot$ are completely convective. However, we find that for higher mass ($\sim 0.07 M_\odot$) stars of the same age, a conductive core might occupy up to $\sim 20\%$ of the mass. This estimate is based on the temperature-density profile of an $n = 3/2$ polytrope. We have not yet, however, calculated fully self-consistent stellar models containing conductive cores. Our estimate of the regions over which conductive cores will form in these low-mass stars depends sensitively on the assumed thermal conductivity and temperature-density profile. Nonetheless, it is important to note that by the time these stars develop significant conductive cores, they are quite degenerate. Hence, the assumption of an $n = 3/2$ polytropic structure is still valid even though the temperature gradient may be much smaller than that needed to support convection near the stellar center. Thus, the principal consequence of the development of a conductive core should be only a slight redistribution of the luminosity as a function of age.

IV. APPLICATIONS

The cooling calculations presented in the previous section have a direct application to the interpretation of observations

of VB 8B, which is reported to have a bolometric luminosity of $\sim 3 \times 10^{-5} L_\odot$ and an effective temperature of ~ 1360 K (McCarthy, Probst, and Low 1985). In Table 2 we list some of the physical properties of our standard models that have luminosities and effective temperatures similar to those of VB 8B (see also NRJ). For brown dwarfs with masses in the range of ~ 0.04 – $0.05 M_\odot$, the cooling tracks pass through ranges of effective temperature and luminosity that closely match those of VB 8B. However, at these masses, the model properties provide a good fit to the observations of VB 8B only for model ages of ~ 4 – 8×10^8 yr. Such ages are young compared to those that might be expected if the VB 8B system were drawn from a random sample of disk-population systems (whose mean age is several billion years; see, e.g., McCarthy, Probst, and Low 1985 for a related discussion). On the other hand, observational selection effects might favor the discovery of such objects when they are young and thus relatively bright. Our $0.06 M_\odot$ model provides perhaps the best overall fit to the properties of VB 8B, with a luminosity close to that observed and a reasonable age of $\sim 1 \times 10^9$ yr. For brown dwarfs of larger mass (~ 0.07 – $0.08 M_\odot$), the ages required to cool to $T_e \approx 1360$ K are even more plausible (~ 2 – 5×10^9 yr); however, we find the luminosities for these stars to be up to $\sim 30\%$ smaller than the observationally inferred value. This discrepancy would be removed if the actual effective temperature of VB 8B were only slightly higher (i.e., ~ 1500 K) than the observationally inferred value, which has an uncertainty of about ± 170 K (McCarthy, Probst, and Low 1985).

We also note that the minor apparent discrepancies between the inferred luminosity and age of VB 8B and the properties of our theoretical models might be removed by invoking models whose masses are just below the minimum main-sequence mass. Such stars may nearly achieve thermal equilibrium for a time comparable to the age of the Galaxy, while maintaining the extremely low effective temperatures that have been reported for VB 8B (DM; Dorman, Chau, and Nelson 1986; Nelson, Rappaport, and Joss 1986c).

We have also utilized our cooling curves to calculate some illustrative theoretical luminosity functions for brown dwarfs. Staller and de Jong (1981) have previously carried out an extensive analysis of such luminosity functions and explored a wide range of assumptions concerning the initial mass function for low-mass stars. However, these authors had access only to earlier cooling curves (Tarter 1975; Stevenson 1978) that were somewhat less complete and accurate than the ones presented in this work.

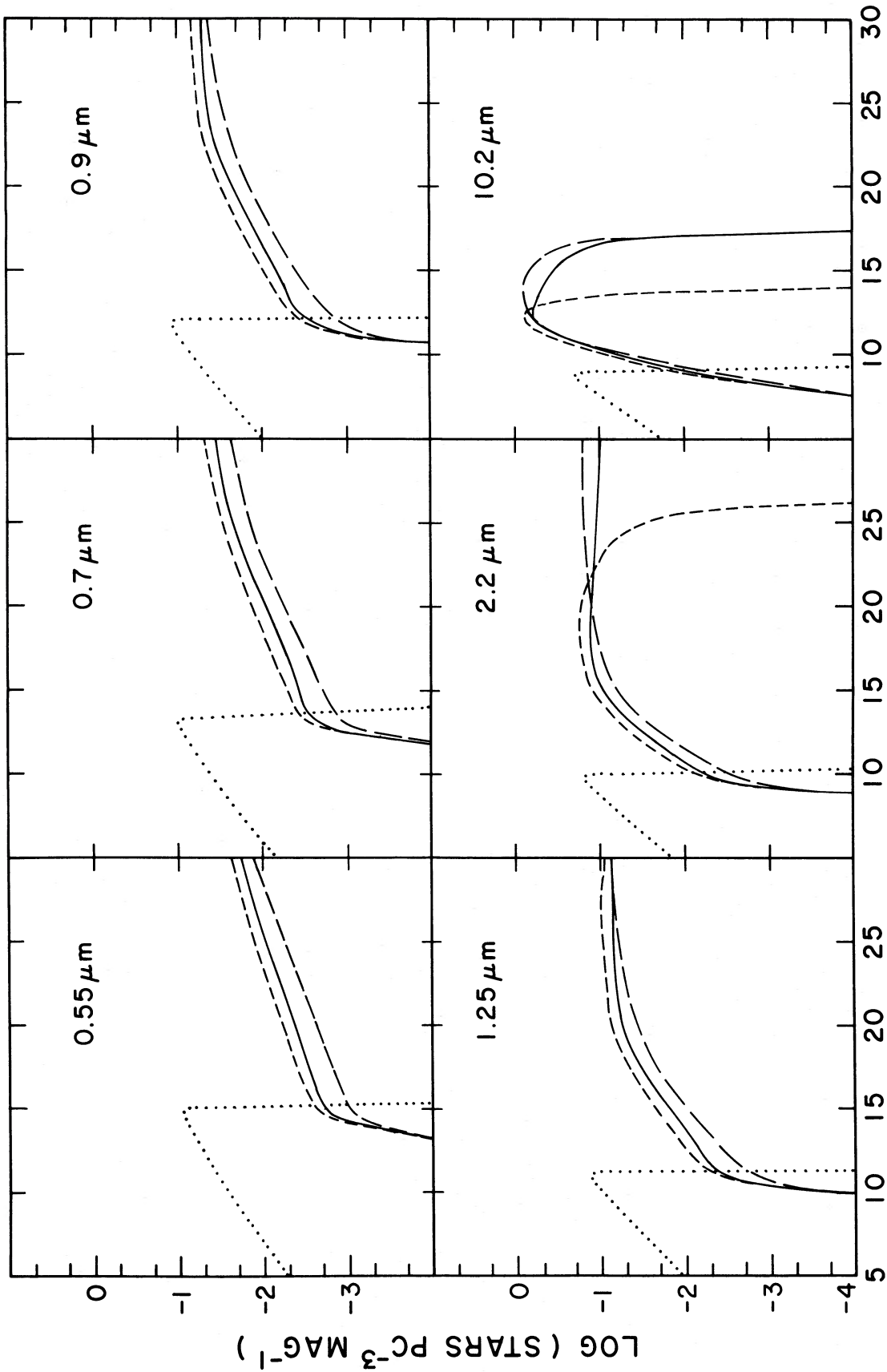
For simplicity, we have arbitrarily adopted a constant rate for the formation of low-mass ($M < 0.08 M_\odot$) stars through-

TABLE 2
MODELS FOR VB 8B^a

$M(M_\odot)$	$R(R_\odot)$	$L(10^{-5} L_\odot)$	$t(10^9 \text{ yr})$	ρ_c	$T_c(10^6 \text{ K})$	D_c^b
0.02.....	0.135	5.62	0.08	57	0.53	2.19
0.03.....	0.116	4.16	0.20	140	0.80	2.53
0.04.....	0.104	3.36	0.43	265	1.06	2.82
0.05.....	0.096	2.85	0.79	430	1.31	3.08
0.06.....	0.090	2.49	1.32	640	1.55	3.33
0.07.....	0.085	2.22	2.19	890	1.79	3.55
0.08.....	0.081	2.01	5.15	1190	2.02	3.78

^a For an assumed effective temperature of 1360 K.

^b Ratio of total perfect gas pressure to ideal gas pressure, evaluated at the stellar center.



ABSOLUTE MAGNITUDE

FIG. 10.—Luminosity functions for brown dwarfs in six standard passbands. In each frame, the long-dashed curve, short-dashed curve, and solid curve correspond to hypothetical initial mass functions given by eqns. (5a), (5b), and (5c), respectively. The initial mass functions have all been normalized to yield a mass density in brown dwarfs of $0.08 M_{\odot} \text{ pc}^{-3}$ at the present epoch. The dotted curves represent the luminosity functions for stars on the zero-age hydrogen-burning main sequence (see text for details).

out the history of the galactic disk, which we take to have an age of 1.5×10^{10} yr. Essentially nothing is known about the initial mass function for stars with $M < 0.08 M_{\odot}$. We have, therefore, chosen the following three illustrative forms for the initial mass function of stars with masses below the end of the hydrogen-burning main sequence:

$$N(M) \propto M^{-2.35} \quad 0.01 M_{\odot} \leq M \leq 0.08 M_{\odot}, \quad (5a)$$

$$N(M) \propto M^{-2.35} \quad 0.03 M_{\odot} \leq M \leq 0.08 M_{\odot}, \quad (5b)$$

$$N(M) \propto M^{-1.5} \quad 0.01 M_{\odot} \leq M \leq 0.08 M_{\odot}, \quad (5c)$$

where $N(M)$ has units of number of stars per mass increment. Below the lower mass limit for each of these initial mass functions we assume that $N(M) = 0$. The lower mass limits are supported by the recent calculations of Boss (1986), who obtained estimates of ~ 0.02 – $0.05 M_{\odot}$ for the minimum protostellar mass that results from hierarchical fragmentation of interstellar clouds. The spectral index of -2.35 in equations (5a) and (5b) is an extrapolation of the power law derived by Salpeter (1955) for more massive stars, while the index of -1.5 in equation (5c) is suggested by the work of Miller and Scalo (1978). For all three functions, we have used a normalization that yields a solar-neighborhood (galactic midplane) mass density of brown dwarfs at the present epoch of $\sim 0.08 M_{\odot} \text{ pc}^{-3}$ (Bahcall 1984).

The results of our calculations of the luminosity functions for brown dwarfs are shown in Figure 10 for six different standard photometric passbands. The definitions of zero magnitude in each passband were taken from Johnson (1966). We also show, for each distribution of brown-dwarf magnitudes, an illustrative curve that represents stars on the zero-age hydrogen-burning main sequence (with $M > 0.085 M_{\odot}$). To generate the zero-age main-sequence luminosity functions, we (i) again adopted a power-law form for the initial mass function, with a spectral index of -2.35 (Salpeter 1955), (ii) normalized the initial mass function so that the mass density of zero-age main-sequence stars in the solar neighborhood is $\sim 0.08 M_{\odot} \text{ pc}^{-3}$, and (iii) utilized the fitting formulae of Whyte and Eggleton (1980) for L and R as functions of M for stars on the lower main sequence.

We draw the following conclusions from the brown-dwarf luminosity functions shown in Figure 10: (i) The three choices of initial mass function produce similar magnitude distributions (within a factor of ~ 2 in space density), except at the longer wavelengths. This is not particularly surprising, since the initial mass functions are all normalized to yield a fixed mass density of brown dwarfs. (ii) As expected, the greater the relative number of higher mass stars implied by a given initial mass function, the greater the predicted space densities of brighter stars. (iii) Our results are in good agreement with those of Staller and de Jong (1981) for the case where they chose the Stevenson (1978) cooling curves and birthrate function that was constant in time. However, Staller and de Jong (1981) find a greater dependence on the assumed slope and lower mass cutoff of the initial mass function than indicated by

our results in Figure 10. This difference results largely from their choice of fixing the luminosity function at a given magnitude, as opposed to our choice of normalizing the initial mass function to yield a specific mass density. (iv) Such luminosity functions can be used to predict specific numbers of stars in various spectral bandpasses that can be observed in the future with the Hubble Space Telescope and SIRTf.

V. CONCLUSIONS

From our evolutionary calculations of brown dwarfs we are able to reach a number of secure conclusions:

1. For brown dwarfs with masses substantially below the end of the hydrogen-burning main sequence (i.e., $\lesssim 0.06 M_{\odot}$), we obtain the following results. (a) The evolution of the effective temperature and bolometric luminosity are fairly well determined, despite the residual uncertainties in the input physics. In particular, we have shown that the evolution is remarkably insensitive to the choice of the atmospheric opacity law at low temperatures and to the amount of mismatch in specific entropy across the stellar envelope. (b) The uncertainties in the effective temperatures for stellar ages up to the age of the Galaxy are typically only 10%. However, as pointed out by a number of workers (e.g., Bahcall 1986; Lunine, Hubbard, and Marley 1986b), there still would be large theoretical uncertainties in the spectral features of such low-temperature stars even if the effective temperatures were known exactly. (c) For stellar ages in excess of $\sim 10^9$ yr, the effective temperatures and luminosities can be reasonably well represented by power-law fitting formulae with $T_e \propto t^{-0.29}$ and $L \propto t^{-1.2}$ (see eqs. [3] and [4]). (d) For ages up to the age of the Galaxy, crystallization and Debye cooling are unlikely to have any significant effect on the evolution.

2. We also find that the minimum mass for a star to attain main-sequence status is moderately sensitive to the assumed input physics, particularly the surface boundary conditions.

3. For the recently discovered brown dwarf VB 8B, we conclude that the theoretically inferred parameters are $M = 0.04$ – $0.08 M_{\odot}$ (see also McCarthy, Probst, and Low 1985), $\rho_c = 300$ – 1300 g cm^{-3} , and $T_c = 1.0$ – $2.0 \times 10^6 \text{ K}$ (see also NRJ). A significant fraction of the pressure support for VB 8B is provided by electron degeneracy. There remain only some minor discrepancies between the models and the observations.

4. Finally, concerning the observability of brown dwarfs as a class, we find that if brown dwarfs account for the local missing mass of the galactic disk (see, e.g., Bahcall 1984), then the theoretical luminosity functions for such objects are reasonably well determined (except for the contribution of stars just below the end of the main sequence). Our luminosity functions indicate that numerous brown dwarfs should be detectable with the Hubble Space Telescope and SIRTf.

We thank J. Lunine, S. Stahler, D. Stevenson, and S. Tremaine for several helpful discussions. One of us (L. A. N.) acknowledges a postdoctoral fellowship from the N.S.E.R.C. of Canada.

REFERENCES

- Alexander, D. R. 1975, *Ap. J. Suppl.*, **29**, 363.
 Alexander, D. R., Johnson, H. R., and Rypma, R. L. 1983, *Ap. J.*, **272**, 773.
 Auman, J. R., Jr. 1969, *Ap. J.*, **157**, 799.
 Bahcall, J. N. 1984, *Ap. J.*, **287**, 926.
 ———. 1986, in *Astrophysics of Brown Dwarfs*, ed. M. Kafatos (Cambridge: Cambridge University Press), in press.
 Bishop, D. M., and Shih, S.-K. 1976, *J. Chem. Phys.*, **64**, 162.
 Bodenheimer, P. 1966, *Ap. J.*, **144**, 103.
 Boss, A. P. 1986, in *Astrophysics of Brown Dwarfs*, ed. M. Kafatos (Cambridge: Cambridge University Press), in press.
 D'Antona, F., and Mazzitelli, I. 1985, *Ap. J.*, **296**, 502 (DM).
 Dorman, B., Chau, W. Y., and Nelson, L. A. 1986, in preparation.
 Gatewood, G. 1976, *Icarus*, **27**, 1.
 Gautier, D., and Owen, T. 1983, *Nature*, **302**, 215.

- Gehrz, R. D., Black, D. C., and Solomon, P. M. 1984, *Science*, **224**, 823.
 Grossman, A. S., and Graboske, H. C., Jr. 1973, *Ap. J.*, **180**, 195.
 Grossman, A. S., Hays, D., and Graboske, H. C., Jr. 1974, *Astr. Ap.*, **30**, 95 (GHG).
 Hansen, J. P. 1973, *Phys. Rev. A*, **8**, 3096.
 Harrington, R. S. 1986, in *Astrophysics of Brown Dwarfs*, ed. M. Kafatos (Cambridge: Cambridge University Press), in press.
 Hayashi, C., and Nakano, T. 1963, *Progr. Theor. Phys.*, **30**, 460.
 Hoxie, D. T. 1970, *Ap. J.*, **161**, 1083.
 Hubbard, W. B. 1973, *Ap. J. (Letters)*, **182**, L35.
 ———. 1986, in *Astrophysics of Brown Dwarfs*, ed. M. Kafatos (Cambridge: Cambridge University Press), in press.
 Hubbard, W. B., and Lampe, M. 1969, *Ap. J. Suppl.*, **18**, 297.
 Hubbard, W. B., and Smoluchowski, R. 1973, *Space Sci. Rev.*, **14**, 599.
 Iben, I., Jr. 1975, *Ap. J.*, **196**, 525.
 Ichimaru, S. 1982, *Rev. Mod. Phys.*, **54**, 1017.
 Johnson, H. L. 1966, *Ann. Rev. Astr. Ap.*, **4**, 193.
 Kumar, S. S. 1963a, *Ap. J.*, **137**, 1121.
 ———. 1963b, *Ap. J.*, **137**, 1126.
 Lippincott, S. L. 1978, *Space Sci. Rev.*, **22**, 153.
 Lunine, J. I., Hubbard, W. B., and Marley, S. 1986a, in *Astrophysics of Brown Dwarfs*, ed. M. Kafatos (Cambridge: Cambridge University Press), in press.
 ———. 1986b, *Ap. J.*, **310**, 238.
 McCarthy, D. W. Jr., Probst, R. G., and Low, F. J. 1985, *Ap. J. (Letters)*, **290**, L9.
 Miller, G. E., and Scalo, J. M. 1978, *Ap. J. Suppl.*, **41**, 513.
 Mould, R. 1976, *Astr. Ap.*, **48**, 443.
 Nelson, L. A., Rappaport, S. A., and Joss, P. C. 1985, *Nature*, **316**, 42 (NRJ).
 ———. 1986a, in *Astrophysics of Brown Dwarfs*, ed. M. Kafatos (Cambridge: Cambridge University Press), in press.
 ———. 1986b, *Ap. J.*, **304**, 231.
 ———. 1986c, in preparation.
 Paczyński, B., and Sienkiewicz, R. 1981, *Ap. J. (Letters)*, **248**, L27.
 Patterson, J. 1984, *Ap. J. Suppl.*, **54**, 443.
 Popper, D. M. 1980, *Ann. Rev. Astr. Ap.*, **18**, 115.
 Probst, R. G. 1977, *A.J.*, **82**, 656.
 Probst, R. G., and Liebert, J. 1983, *Ap. J.*, **274**, 245.
 Rappaport, S., and Joss, P. C. 1984, *Ap. J.*, **283**, 232.
 Rappaport, S., Joss, P. C., and Webbink, R. F. 1982, *Ap. J.*, **254**, 616 (RJW).
 Rappaport, S., Verbunt, F., and Joss, P. C. 1983, *Ap. J.*, **275**, 713.
 Salpeter, E. E. 1955, *Ap. J.*, **121**, 161.
 Slattery, W. L., Doolen, G. D., and DeWitt, H. E. 1980, *Phys. Rev. A*, **21**, 2087.
 ———. 1982, *Phys. Rev. A*, **26**, 2255.
 Stahler, S. W., Palla, F., and Salpeter, E. E. 1986, *Ap. J.*, **302**, 590.
 Staller, R. F. A., and de Jong, T. 1981, *Astr. Ap.*, **98**, 140.
 Stevenson, D. J. 1978, *Proc. Astr. Soc. Australia*, **3**, 227.
 ———. 1986, in *Astrophysics of Brown Dwarfs*, ed. M. Kafatos (Cambridge: Cambridge University Press), in press.
 Tarter, J. 1975, Ph.D. thesis, University of California, Berkeley.
 van de Kamp, P. 1969, *Pub. A.S.P.*, **81**, 5.
 ———. 1975, *Ann. Rev. Astr. Ap.*, **13**, 295.
 Whyte, Ch. A., and Eggleton, P. P. 1980, *M.N.R.A.S.*, **190**, 801.
 Zapsolsky, H. S., and Salpeter, E. E. 1969, *Ap. J.*, **158**, 809.

P. C. JOSS: Room 6-203, M.I.T., Cambridge, MA 02139

L. A. NELSON: Room 6-214, M.I.T., Cambridge, MA 02139

S. A. RAPPAPORT: Room 37-551, M.I.T., Cambridge, MA 02139